Surface-stress-induced phase transformation in metal nanowires

JIANKUAI DIAO*, KEN GALL AND MARTIN L. DUNN
Department of Mechanical Engineering, University of Colorado, Boulder, Colorado 80309, USA
*e-mail: diao@colorado.edu

Published online: 7 September 2003; doi:10.1038/nmat977

Several researchers[1–8] have demonstrated, through experiments and analysis, that the structure and properties of nanometre-scale materials can be quite different to those of bulk materials due to the effect of surfaces. Here we use atomistic simulations to study a surface-stress-induced phase transformation in gold nanowires. The emergence of the transformation is controlled by wire size, initial orientation, boundary conditions, temperature and initial cross-sectional shape. For a <100> initial crystal orientation and wire cross-sectional area below 4 nm^2, surface stresses alone cause gold nanowires to transform from a face-centred-cubic structure to a body-centred-tetragonal structure. The transformation occurs roughly when the compressive stress caused by tensile surface-stress components in the length direction exceeds the compressive stress required to transform bulk gold to its higher energy metastable crystal structure.

Unique structures in low-dimensional nanometre-scale materials are driven by the tendency of surfaces to reduce their surface energy. Large tensile surface stresses exist in the {100} surfaces of the end-of-series 5*d* elements Ir, Pt and Au, and cause the {100} surfaces of those metals to contract and reconstruct into a hexagonal close-packed lattice, in contrast with the underlying bulk square lattice[9–13]. As the scale of materials reduces to nanometres, the tendency of surfaces to reduce their surface energy may drive structural change beyond the surface layers into the 'bulk'. The reorientation of face-centred-cubic (f.c.c.) {100} gold films into {111} films has been observed when the film thickness was less than eight atomic layers[1]. By molecular dynamics simulation, it was demonstrated[2] that the aforementioned reorientation is universal to transition metals including both the 5*d* and 4*d* series. A hexagonal prism structure has been proposed[3] for a 2-nm-thick Au nanowire with an initial orientation of <110> based on high-resolution transmission electron microscopy observations. The surface of the wire reconstructed to have a hexagonal closed-packed lattice, and the core of the wire kept its initial f.c.c. structure. It was also proposed[4] that as the <110> Au nanowires are thinned further to less than 1.5 nm in diameter, they form a helical multishell structure composed of coaxial tubes. 'Weird' structures were predicted[5] for Al and Pb nanowires, including the helical multishell structure, from molecular dynamics simulations. The stability of a single-tube Au nanowire was confirmed through density-functional calculations[6]. Clusters of Ag[7] and other metals[8] have been observed to form an icosahedral shape below a critical size. The icosahedral shape is favoured because it has only {111} surfaces, the lowest in surface energy.

We investigate the energetics and structure of Au nanowires with an initial <100> orientation and a square cross-section. The tensile surface-stress components in the length direction cause a significant compressive stress–strain in the core of the wire, ultimately inducing a phase transformation from an f.c.c. structure into a body-centered-tetragonal (b.c.t.) structure below a cross-sectional area near 4 nm^2. Wires with initial <111> and <110> orientations did not undergo the f.c.c.–b.c.t. phase transformation. The structural transformation has not been discovered in previous studies on nanowires[5–8] because of key differences in the initial orientations, initial cross-sectional shape, and boundary conditions of the wires. In fact, our simulations predict the helical multishell structure in wires with initial <110> and <100> orientations, in agreement with previous molecular dynamics study[5], when the same wire size, boundary conditions and annealing procedures were used. At larger wire sizes, our simulations predict the reorientation and reshaping of <100> wires into <110> wires with {111} surfaces, in line with experimental observation[3] (see Supplementary Information).

We used the modified embedded atom method (MEAM) with Au potential developed previously[14,15]. Au [100] nanowires with a square cross-section and surface orientations of [100], [010] and [001] were created with initial atomic positions corresponding to the bulk f.c.c. crystal. The original length of the wires was 32 nm and the cross-sectional area was varied. The wires were then relaxed to a minimum energy state in a molecular static framework at 0 K using the conjugate gradient method. Free boundary conditions were used in all directions.

Owing to the tensile surface-stress components in the length direction, the wires contract on relaxation. For wires with an initial cross-sectional area larger than 1.83 nm × 1.83 nm, the contraction is less than 4% and is realized by nonlinear elastic compression of the wire. However, when the initial cross-sectional area is equal to or less than 1.83 nm × 1.83 nm, the contraction in the length direction exceeds 30%. Figure 1a shows the unrelaxed and relaxed configurations of the 1.83 nm × 1.83 nm wire with the atoms coloured by a centrosymmetry parameter[16], a measure of the degree to which a given atom is locally a centre of inversion symmetry. This parameter is zero for a perfect f.c.c. crystal and becomes non-zero at structural defects including crystal surfaces. Figure 1b,c,d shows the cross-sections at the centre region of the unrelaxed and relaxed 1.83 nm × 1.83 nm nanowire, observed from the *x*, *y* and *z* directions, respectively. Only two adjacent lattice planes of atoms are shown as the lattice planes repeat in an ABAB stacking sequence.

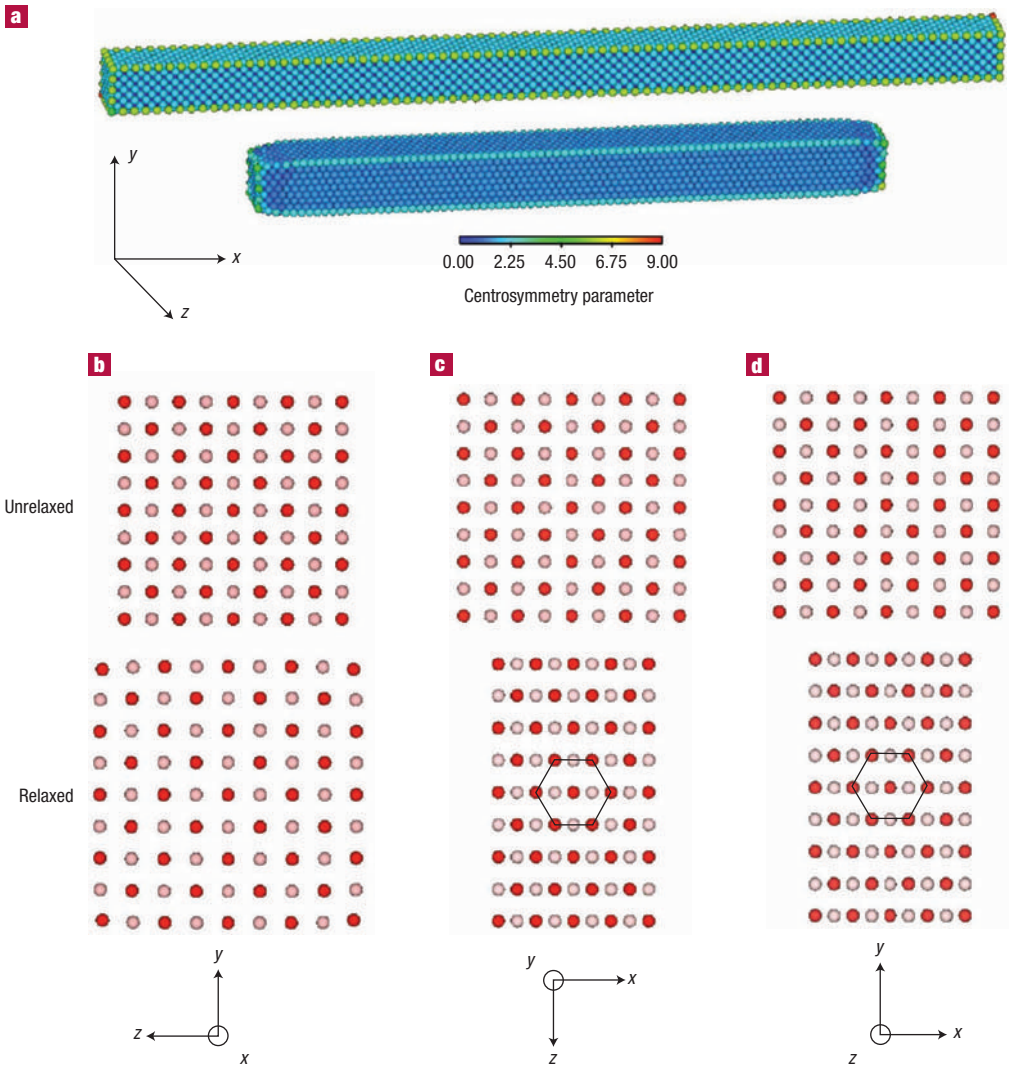

Figure 1 The phase transformation in the 1.83 nm × 1.83 nm <100> wire. a, Unrelaxed and relaxed configurations of the wire. Atoms are coloured according to the centrosymmetry parameter. **b**, **c**, **d**, Cross-sections at the centre regions of the unrelaxed and relaxed wires, observed from *x*, *y* and *z* directions respectively, only two adjacent lattice planes of atoms are shown, and atoms in different lattice planes are shown in different colours. In **c** and **d** only partial regions of the wires are shown in the *x* direction.

In Fig. 1b,c,d, the atoms in A and B planes are shown in different colours, and are not coloured by the centrosymmetry parameter.

Crystallographic arguments show that a phase transformation occurs from the original f.c.c. structure to a b.c.t. structure for wires with initial cross-sectional area equal to or less than 1.83 nm × 1.83 nm. Consider a unit cell of the unrelaxed 1.83 nm × 1.83 nm wire, which is an f.c.c. cell with a lattice constant of 4.07 Å. After relaxation, owing to the contraction in the *x* direction, the length of the cell in the *x* direction becomes 2.824 Å. Meanwhile the wire expands in the *y* and *z* directions on relaxation and the length of the cell in those directions become 4.758 Å. The contraction and expansions change the structure of the wire from the original f.c.c. to b.c.t. with lattice parameters of $a = 4.758/\sqrt{2}$ Å and $c = 2.824$ Å. We should mention that the values of the lattice constants are averaged values over all unit cells except those at ends of the wire. Owing to the phase transformation, the side surfaces of the relaxed wire are all hexagonally close-packed and contracted 1.9% in the *x* direction and 4.5% in the *y* and *z* directions with respect to an f.c.c. Au {111} plane lattice.

We also conducted molecular dynamic simulations at 100 K on the 1.83 nm × 1.83 nm wire to study the dynamics of the phase transformation with free boundary conditions identical to those in the static simulations. Figure 2 shows the dynamic progression of the phase transformation in the 1.83 nm × 1.83 nm wire. The phase transformation nucleates from the ends of the wire, and propagates toward the centre at an average speed of 347 m s^{-1}. This propagation speed is about one order of magnitude slower than the longitudinal sound-wave speed in gold. The phase transformation front represents a coordinated shift of the atoms from the f.c.c. lattice to the b.c.t. lattice. We verified the stability of the b.c.t. nanowire by simulated annealing. The temperature was raised from 100 K to 600 K gradually, kept at 600 K for 1 ns (10^6 timesteps) and then lowered to 100 K gradually. The b.c.t. wire kept its structure during the entire annealing process. The molecular dynamic simulation is of particular interest, as it demonstrates how the local minimum energy state predicted by the static simulation is achieved by the nucleation and propagation of a phase transformation throughout the wire. As is the case with many

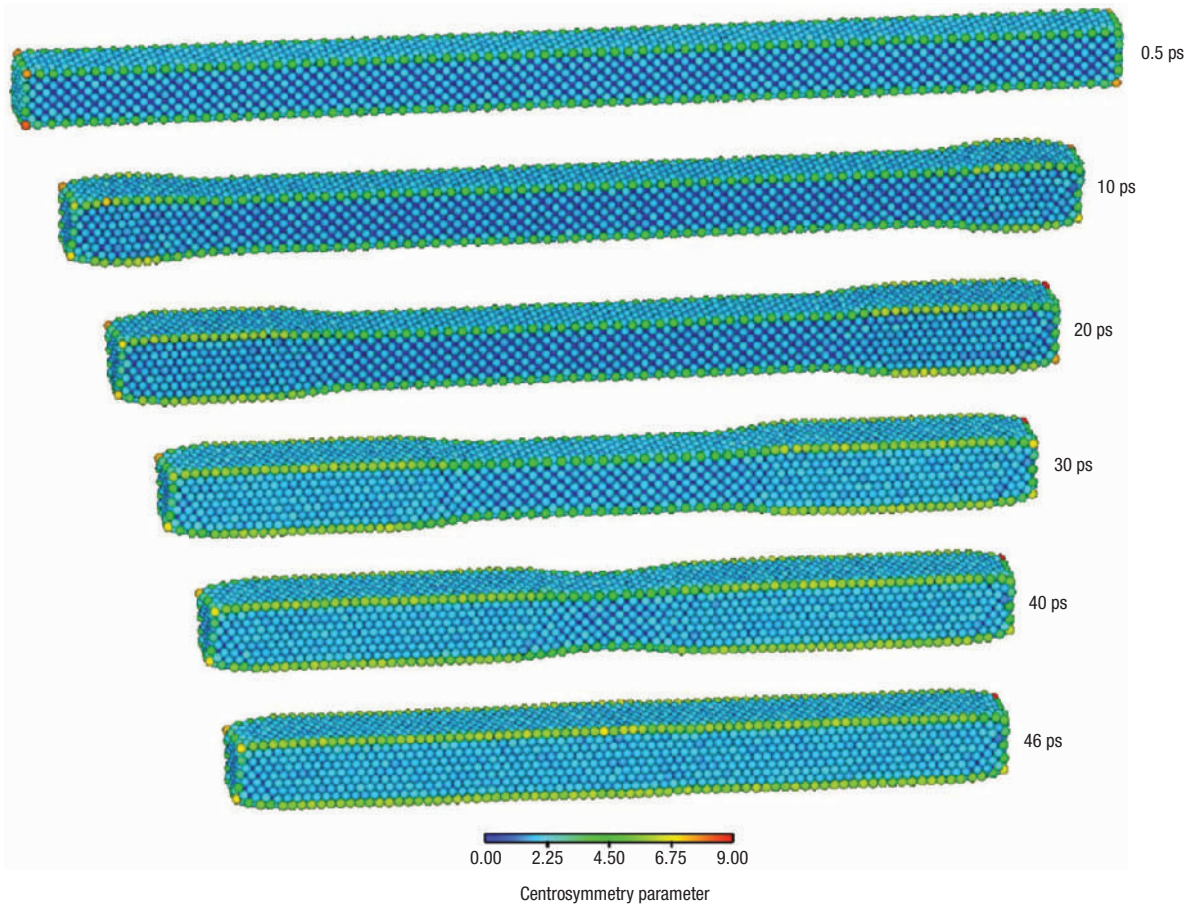

Figure 2 The dynamic progression of the phase transformation in the 1.83 nm × 1.83 nm nanowire at 100 K. Atoms were assigned initial velocities according to a Boltzmann distribution appropriate for 100 K. Frames shown are configurations of the wire at 0.5, 10, 20, 30, 40 and 46 ps. Atoms are coloured according to centrosymmetry parameter.

solid-state phase transformations, the nucleation is heterogeneous, occurring at the ends of the wire in a region with elevated non-uniform stress. The heterogeneous nature of the transformation implies that it will be strongly dependent on boundary conditions and local structural features.

The surface stress can be viewed as the driving force for the phase transformation. A simplified continuum model of a nanowire, considering only the surface-stress components in the length direction, can be constructed by subjecting a bulk wire to an externally applied force to create a compressive stress. Given the stress required to induce the phase change in the bulk wire, and the surface-stress magnitude, the simplified model can be used to estimate the critical nanowire size that will cause the transformation. To estimate this critical nanowire size, we performed uniaxial compression-loading in the [100] direction of bulk gold under force control. Periodic boundary conditions were used in the [100], [010] and [001] directions to emulate bulk gold. Force was applied in the [100] direction and the periodic lengths in all the three directions were allowed to adjust to the applied load.

Figure 3 shows the compressive stress–strain curve for bulk gold. As the compression load is increased, the deformation initially follows the path (1), at a critical stress of 1.6 GPa, the deformation jumps from path (1) to path (2), and at a critical stress of 3.7 GPa, the deformation jumps from path (2) to path (3). Throughout the entire loading process, the tetragonal symmetry is maintained, that is, the deformation is along the Bain path[17]. Two distinct structures were observed in paths (2) and (3). We unloaded the force from the paths (2) and (3) to investigate the resulting stress-free structures. They are both b.c.t., one with $a = 4.260/\sqrt{2} = 3.012$ Å and $c = 3.595$ Å, the other with $a = 4.813/\sqrt{2} = 3.404$ Å and $c = 2.856$ Å. We will refer to those two new structures as b.c.t.1 and b.c.t.2, respectively, in the following text. The average lattice constants of the transformed nanowires in Figs 1a and 2 are about 1% smaller in both a and c than those of the bulk b.c.t.2 structure due to the tensile surface stresses on the transformed wires. Consequently, the static and dynamic simulations presented in Figs 1 and 2 only show evidence of the b.c.t.2 structure. We explain this apparent discrepancy in the following text.

Using a method similar to that of Streitz *et al.*[18], we calculated the surface-stress components for the unstrained f.c.c., b.c.t.1 and b.c.t.2 structures for various crystallographic planes and orientations (Table 1). The tensile surface-stress components in the length direction on the four side surfaces of a nanowire induce a compressive stress in the nanowire. At equilibrium, the magnitude of the induced compressive stress can be estimated as $\sigma = 4fl/A$, where f is the surface-stress component, l is the width of a nanowire (the length over which the surface-stress component acts), and A is the cross-sectional area. In a relaxed nanowire, the tensile surface-stress component and the induced compressive stress balance each other and the average stress is zero over the cross-sectional area. When the induced compressive stress in a

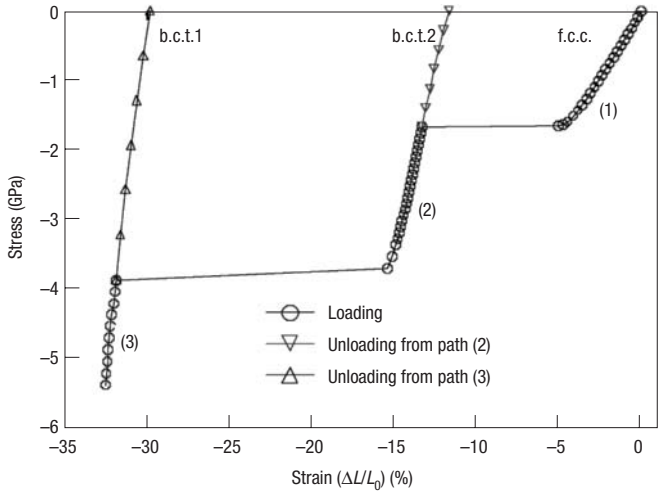

Figure 3 Uniaxial stress–strain curve of bulk gold under compression and unloading curves from paths (2) and (3) (see text). The loading and unloading are in the [100] direction.

nanowire reaches the critical compressive stress from the compression loading of bulk gold, phase transformation occurs. Based on the simplified model, considering only the surface-stress component in the length direction, the critical cross-sectional size for the f.c.c. to b.c.t.1 transformation is 2.56 nm × 2.56 nm, at which size the magnitude of the induced compressive stress is 1.6 GPa, the critical compressive stress required for the phase change from f.c.c. to b.c.t.1 in bulk gold. However a slightly smaller critical size of 1.83 nm × 1.83 nm is observed in the static simulation, due to the fact that there are tensile surface-stress components in the transverse directions of actual nanowires. The tensile surface-stress components in transverse directions constrain the expansion of the wire in the transverse directions and hinder the phase transformation, lowering the actual wire size necessary for the transformation.

We have shown that the surface stresses of the f.c.c. 1.83 nm × 1.83 nm wire are large enough to induce the wire to transform from f.c.c. to b.c.t.1. However, in both the static and dynamic simulations, the wire ultimately transforms to the b.c.t.2 structure. The b.c.t.1 wire is not observed in the simulations because its surface-stress component in the length direction is considerably higher than that of the f.c.c. wire, 2.85 J m^{-2} versus 1.03 J m^{-2}, respectively (Table 1). The magnitude of the compressive stress induced by the surface-stress component in the length direction of the b.c.t.1 wire is 5.95 GPa. This stress is much larger than the critical stress of 3.72 GPa required to induce phase transformation from b.c.t.1 to b.c.t.2 in bulk gold. Consequently, the surface stresses induce two successive phase transformations in the 1.83 nm × 1.83 nm wire. We should mention that in dynamic simulations at lower temperature (10 K) we did observe b.c.t.1 structure, the f.c.c. wire transforms first to the b.c.t.1 wire, and then the b.c.t.1 wire transforms to the b.c.t.2 wire.

We have examined the energetics of the phase transformation using static simulations. The calculated cohesive energies for bulk f.c.c., b.c.t.1 and b.c.t.2 gold are listed in Table 1 along with the respective surface energies. We see that bulk b.c.t.1 and b.c.t.2 gold have higher energies per atom than the bulk f.c.c. gold, but lower surface energies for the specific surfaces of the wire. The total energies of f.c.c. wires will crossover those of the b.c.t.1, and b.c.t.2 wires as the wire size decreases (The total energy of the b.c.t.2 wire is always lower than that of the b.c.t.1 wire). We estimated that when the cross-sectional area of an f.c.c. wire is less than 30.1 nm × 30.1 nm, the corresponding b.c.t.2 wire has the lowest total energy. However, in our static simulations we do not predict the transformation to b.c.t.2 structure until a much smaller wire size. The phase transformation will not occur just because the total energy of the b.c.t.2 wire is lower than that of the corresponding f.c.c. wire. Energy barriers exist between the f.c.c. and the corresponding b.c.t.2 wires. For wires with cross-sectional area equal to and less than 1.83 nm × 1.83 nm, the surface stresses alone can overcome the energy barriers, as seen in the static simulation. For wires with cross-sectional area in between 1.83 nm × 1.83 nm and 30.1 nm × 30.1 nm, the surface stresses alone cannot overcome the energy barriers. The addition of thermal vibrations may help to overcome energy barriers. For example, we observed phase transformation in the dynamic simulation of a 2.65 nm × 2.65 nm wire at an elevated temperature of 300 K.

Table 1 The surface-stress components and surface energies of f.c.c., b.c.t.1 and b.c.t.2 gold, for surfaces and orientations corresponding to those of the nanowires, along with the cohesive energies of bulk gold. Indices of directions and planes are given in the f.c.c. and b.c.t. coordinate systems respectively.

Crystal structure	Cohesive energy (eV)	Plane i	Surface energy (J m^{-2})	Direction j	Surface stress F_{ij} (J m^{-2})
f.c.c.				All	
$a = c = 4.07$ Å	3.930	{100}	1.04	(isotropic)	1.03
b.c.t.1					
$a = 3.012$ Å				[0 0 1]	2.85
$c = 3.595$ Å	3.923	{110}	0.95	<110>	1.60
b.c.t.2					
$a = 3.404$ Å				[0 0 1]	1.52
$c = 2.856$ Å	3.924	{110}	0.69	<110>	1.54

Received 15 May 2003; accepted 12 August 2003; published 7 September 2003

References

1. Kondo, Y., Ru, Q. & Takayanagi, K. Thickness induced structural phase transition of gold nanofilm. *Phys. Rev. Lett.* **82,** 751–754 (1999).
2. Hasmy, A. & Medina, E. Thickness induced structural transition in suspended fcc metal nanofilms. *Phys. Rev. Lett.* **88,** 096103 (2002).
3. Kondo, Y. & Takayanagi, K. Gold nanobridge stabilized by surface structure. *Phys. Rev. Lett.* **79,** 3455–3458 (1997).
4. Kondo, Y. & Takayanagi, K. Synthesis and characterization of helical multi–shell gold nanowires. *Science* **289,** 606–608 (2000).
5. Gülseren, O., Ercolessi, F. & Tosatti, E. Noncrystalline structures of ultrathin unsupported nanowires. *Phys. Rev. Lett.* **80,** 3775–3778 (1998).
6. Tosatti, E., Prestipino, S., Kostlmeier, S., Dal Corso, A. & Di Tolla, F. D. String tension and stability of magic tip-suspended nanowires. *Science* **291,** 288–290 (2001).
7. Hall, B. D., Flüeli, M., Monot, R. & Borel, J.–P. Multiply twinned structures in unsupported ultrafine silver particles observed by electron diffraction. *Phys. Rev. B* **43,** 3906–3917 (1991).
8. Marks, L. D. Surface structure and energetics of multiply twinned particles. *Philos. Mag. A* **49,** 81–93 (1984).
9. Van Hove M. A. *et al.* The surface reconstructions of the (100) crystal faces of Iridium, Platinum and Gold. *Surf. Sci.* **103,** 189–217 (1981).
10. Yamazaki K., Takayanagi, K., Tanishiro, Y. & Yagi, K. Transmission electron microscope study of the reconstructed Au(100) surface. *Surf. Sci.* **199,** 595–608 (1988).
11. Fiorentini, V., Methfessel, M. & Schoffler, M. Reconstruction mechanism of fcc transition metal (001) surfaces. *Phys. Rev. Lett.* **71,** 1051–1054 (1993).
12. Binnig, G. K., Rohrer, H., Gerber, Ch. & Stoll, E. Real-space observation of the reconstruction of Au(100). *Surf. Sci.* **144,** 321–335 (1984).

13. Gibbs, D., Ocko, B. M., Zehner, D. M. & Mochrie S. G. J. Absolute x-ray reflectivity study of the Au(100) surface. *Phys. Rev. B* **38,** 7303–7310 (1988).
14. Baskes, M. I. Modified embedded-atom potentials for cubic materials and impurities. *Phys. Rev. B* **46,** 2727–2742 (1992).
15. Baskes, M. I., Angelo, J. E. & Bisson, C. L. Atomistic calculations of composite interfaces. *Model. Simul. Mater. Sci. Eng.* **2,** 505–518 (1994).
16. Kelchner, C. L., Plimpton, S. J. & Hamilton, J. C. Dislocation nucleation and defect structure during surface indentation. *Phys. Rev. B* **58,** 11085–11088 (1998).
17. Hahn, E., Kampshoff, E., Wälchli, N. & Kern, K. Strain driven fcc-bct phase transition of pseudomorphic Cu films on Pd(100). *Phys. Rev. Lett.* **74,** 1803–1806 (1995).
18. Streitz, F. H., Cammarata, R. C. & Sieradzki, K. Surface-stress effects on elastic properties. I. Thin metal films. *Phys. Rev. B* **49,** 10699–10706 (1994).

Acknowledgements

The work was supported by Sandia National Laboratories and the National Science Foundation, USA. The authors thank Jon Zimmerman for his insightful discussions and guidance.
Correspondence and requests for materials should be addressed to J.D.
Supplementary Information accompanies the paper on http://www.nature.com/naturematerials

Competing financial interests

The authors declare that they have no competing financial interests.